Border Detection of Melanoma Skin Lesions on a Single System on Chip (SoC)

Peyman Sabouri Hamid GholamHosseini John Collins

Department of Electrical and Electronic Engineering, Auckland University of Technology
Auckland, New Zealand

{psabouri, hgholamh, jcollins}@aut.ac.nz

Received 23 August 2013; Revised 20 October 2013; Accepted 16 December 2013

Abstract. Real-time medical vision systems using single system on chip (SoC) can be employed for early diagnosis of melanoma. This paper presents, a basic border detection algorithm developed based on ZYNQ-7000 SoC, using VIVADO High Level Synthesis (HLS) tool. We take the advantage of accelerating an embedded system design on a single SoC, which offers the required features for real-time processing of skin cancer images. Our ultimate aim is to develop novel methods to detect melanoma more accurately and faster and implement the algorithms on portable vision systems for medical imaging applications with high resolution and performance. Different edge detection approaches such as Sobel, Kirsch, Canny and LoG have been implemented on ZYNQ-7000 for border detection of skin lesions, which can be used in early diagnosis of melanoma. The results show that the extended 5×5 canny edge detection algorithm implemented on the proposed embedded platform has better performance in comparison with other reported methods. The performance evaluation of this approach has shown good processing time of 60 fps for real time applications.

Keywords: Border detection, Edge detection, Medical imaging, ZYNQ-7000, System on Chip

Received 23 August 2013; Revised 10 November 2013; Accepted 16 December 2013

1 Introduction

To date, skin cancers have been one of the most common form of cancers [1]. Typically, skin cancers are divided into two main categories: melanoma and non-melanoma. While melanoma is the most dangerous one, it is curable at early stage of development. Therefore, early diagnosis of melanoma can significantly decrease the morbidity, death and cost of the medications [2]. Non-invasive methods for diagnosis of skin tumours can significantly help early detection of the malignant melanoma and can replace biopsy. Furthermore, due to fast growing of computer aided diagnosis (CAD) systems, there has been a great opportunity to develop portable vision systems for medical imaging applications with high resolution and performance. There are several non-invasive approaches that have been applied on pigmented skin lesion (PSL) image based using different image processing and computer vision techniques [3]. Multi-spectral and hyper-spectral imaging systems have led to renewed interest in diagnosis of melanoma [4, 5]. Dermoscopy is also another non-invasive method for diagnosis of PSLs Although this device illustrates features of PSLs, it is still a challenging task for dermatologist to diagnose melanoma from other skin lesions [6]. A considerable amount of literature has been published on computer aided diagnosis (CAD) of melanoma based on dermoscopy images [3]. Image processing techniques can be applied to the collected dermoscopy images for better diagnosis of melanoma as a second opinion of dermatologists. Image features such as Asymmetry, Border irregularity, Colour variation and regions with Diameter greater than 6mm (ABCD rule) can be extracted using high performance image processing techniques [7]. Recent studies have reported that computer aided diagnosis of melanoma is feasible using RGB clinical images with sensitivity of 80-94% and specificity of 46-95% [8]. A clinical image scene is an image that a clinician observes with naked eye. The dataset can be collected in affordable cost using online resources[8, 9]. Furthermore, RGB clinical image can be used with the state-of-the-art embedded systems as a portable solution with affordable cost to investigate and record skin lesion evolution.

The aim of our study is to investigate and develop novel methods to detect melanoma using efficient medical vision system. The developed algorithms can be implemented on the advanced embedded platforms such as smart-phones, CPUs or a System on Chip (SoC) like ZYNQ-7000 (XILINX). The proposed algorithms are mainly consists of four stages: (1) pre-processing of lesion images in order to enhance the image dataset, (2) lesion border detection to remove the background and outline the lesion border, (3) feature extraction and (4) classification.

This paper has been divided into four sections. Following the introduction, the proposed processing system is described; the basic concept of border detection of skin lesion images is given in section three; section four and five deal with the experimental results and conclusion.

2 Proposed System

High speed image and video processing is becoming increasingly important in medical imaging. Advances in embedded systems and their applications in medical imaging realm are growing fast. However, the limitation of system development on a single platform such as single digital signal processor (DSP) or field programmable gate arrays (FPGA) is a major concern for designing complex systems. Moreover, each platform has its advantages and trade-offs based on the nature of the algorithm, performance requirement, power consumption, cost, productivity, flexibility and design cycle time. One of the recent products from Xilinx, ZYNQ-7000, can be considered as a promising solution to overcome these challenges. The ZYNQ-7000 consists of a dual-core ARM processor which is surrounded by 7-series Xilinx FPGA based on 28 nm technology. The close integration between processing system and programmable logic provides the flexibility of ASIC technology and performance of FPGA technology on a single System on Chip (SoC) [10]. The state-of-the-art ZYNQ-7000 system on chip may be a suitable solution for designing handheld medical imaging systems for skin cancer detection. Fig. 1 shows the block diagram of the proposed system that implemented on the ZYNQ-7000.

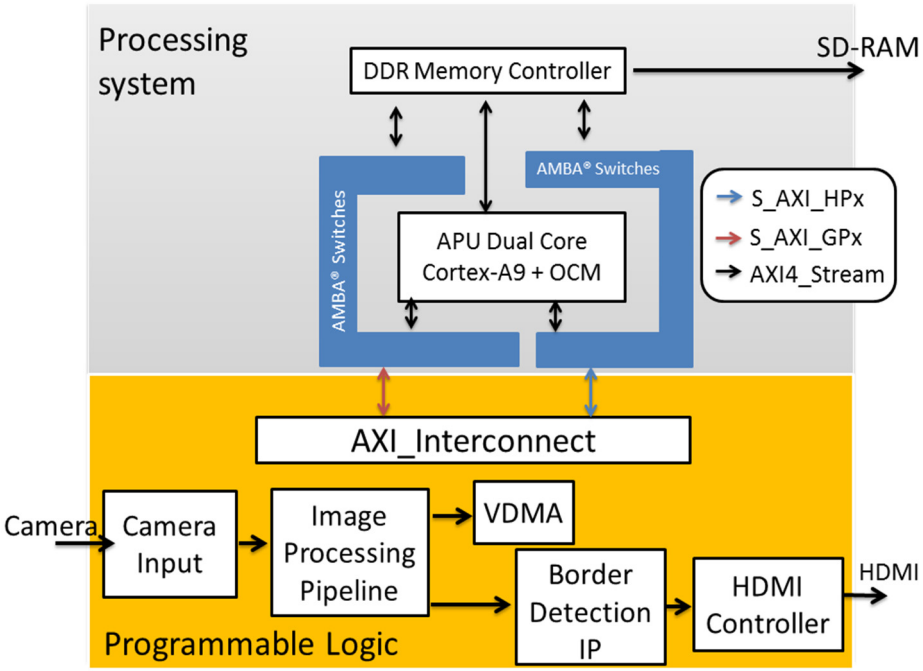

Fig. 1. The block diagram of the proposed system implemented on ZYNQ-7000.

Image processing pipeline block consists of several pre-defined XILINX video IP cores such as defective pixel removal, de-mosaic, colour correction matrices and the border detection IP block which describes in the following section. In order to generate the border detection IP, first we used OpenCV functions for evaluation of the proposed algorithms and then VIVADO HLS software is used to convert C to synthesizable FPGA codes automatically. However, more IPs such as feature extraction and image classification can be developed and added to the system for the skin cancer detection application.

Unlike the traditional FPGA design flows, HLS can improve design quality, accelerate the design and verification tasks by applying optimal synthesis directives to transform C/C++/SystemC code specifications to register transfer level (RTL) implementation [11, 12]. Although C code is used for implementation of the algorithm, several directives such as DataFlow, memory/interface, and for loop optimisations [13] are applied to obtain the

required performance and area utilisation in the programmable logic. Functional verification of the edge detection IP is done using C++ test benches to significantly reduce the development time during the functional verification stage.

3 Border Detection

Border detection plays an important role in the automatic diagnosis of skin cancer. A number of border detection algorithms for segmentation of PSLs either based on dermoscopy images or clinical images have been developed [3]. The more relevant algorithms for hardware implementation are: edge detection [7], active contours [14], thresholding [15], gradient vector flow [16], and hybrid thresholding on optimal colour channels [17]. Although, comparing the accuracy of current methods is out of the scope of this article however, the performance analysis of previous works can be found in [18, 19]. The presence of artefacts such as hairs and specular reflections in skin images may lead to deficient border detection result [20]. Therefore, image pre-processing is an important step for automate diagnosis of melanoma. Fig. 2 illustrates the flowchart of the proposed border detection algorithm. At first, RGB-colour image is converted to Hue/Saturation/Value (HSV) colour space. Pre-processing step is done using morphological filters such as median, erosion and dilation over the image for noise filtering. Afterward, edge detection is applied to the value (intensity) component of the image using 5×5 canny operation to detect outline of skin lesion. It was observed that the images used in this work did not include great quantity of hair artefact.

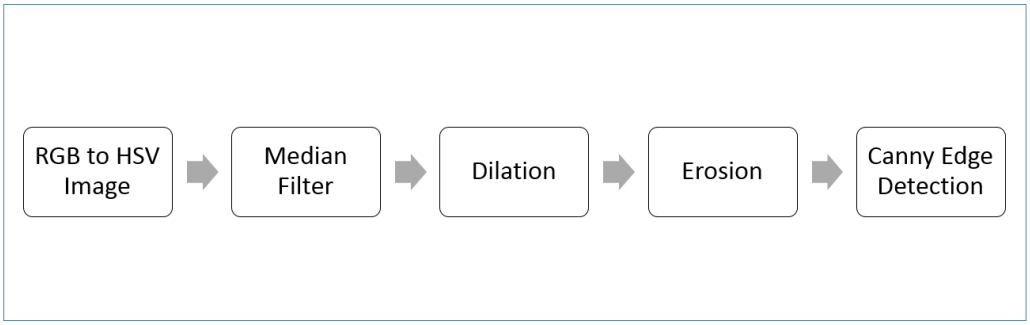

Fig. 2. Flowchart of the border detection algorithm.

Edge detection algorithm used in image analysis with the aim of detection of boundaries between objects and the background in grey level images. Although there are many approaches for edge detection and object recognition in medical imaging, the calculation of the gradient level value for each pixel using a matrix of neighbouring masks and comparing this value with a given threshold, is a common approach. If the calculated value is greater than the threshold, the pixel is considered as an edge. The most important categories of edge detection algorithms are as follows [21]:

- Gradient edge detectors (first derivative such as Sobel, Prewitt and Kirsch)
- Zero crossing (second derivative)
- Laplacian of Gaussian (LoG)
- Gaussian edge detectors (such as Canny)
- Coloured edge detectors

In this work, Sobel, Kirsch, LoG and Canny edge detectors were chosen for border detection of skin cancer images. It was found that 3×3 filters, which are normally used in edge detection methods, are extremely localized. To obtain a better performance, the extended edge operators (5×5 filters) were used to cover more surrounding pixels [22]. This operation involves convolving two 5x5 kernels with a matching 5x5 portion of the image for intensity (value) component. When the convolutions are completed the two kernels are moved one pixel to the right and the process repeated until the full width of the image file is processed. The two kernels are then shifted down one pixel and shifted to the left most edge of the image file. This process is repeated until the end of the image file is reached.

The kernel will always be an odd, but symmetrical dimension, such as three by three, five by five etc.

When using a 5x5 kernel the four pixels closest to the edges will not be fully processed and so any edges will not be fully revealed as the kernel matrix must always be within the bounds of the image file.

The purpose of convolving the kernel with a section of the image file is to compute an approximation of the derivative – one for horizontal, and one for vertical. The resulting derivative gives an approximation of the gradient of the image at that point. This in turn indicates an edge, where the gradients change. The abruptness of this change is measured against a threshold. If the resulting convolution is greater than the threshold then it is deemed to be an edge. The actual kernel values for edge detection operations are set out in the following.

The Sobel operator consists of two vertical and horizontal kernel components, which can be obtained by 3×3 vertical and horizontal kernels (equation (1)).

$$\mathbf{G_x} = \begin{bmatrix} \mathbf{-1} & \mathbf{0} & \mathbf{+1} \\ \mathbf{-2} & \mathbf{0} & \mathbf{+2} \\ \mathbf{-1} & \mathbf{0} & \mathbf{+1} \end{bmatrix}, \mathbf{G_y} = \begin{bmatrix} \mathbf{+1} & \mathbf{+2} & \mathbf{+1} \\ \mathbf{0} & \mathbf{0} & \mathbf{0} \\ \mathbf{-1} & \mathbf{-2} & \mathbf{-1} \end{bmatrix} \quad (\mathbf{1})$$

As mentioned above, the Gx and Gy Kernels are extended to 5×5 masks (equation (2)).

$$\mathbf{G_x} = \begin{bmatrix} \mathbf{2} & \mathbf{2} & \mathbf{4} & \mathbf{2} & \mathbf{2} \\ \mathbf{1} & \mathbf{1} & \mathbf{2} & \mathbf{1} & \mathbf{1} \\ \mathbf{0} & \mathbf{0} & \mathbf{0} & \mathbf{0} & \mathbf{0} \\ \mathbf{-1} & \mathbf{-1} & \mathbf{-2} & \mathbf{-1} & \mathbf{-1} \\ \mathbf{-2} & \mathbf{-2} & \mathbf{-4} & \mathbf{-2} & \mathbf{-2} \end{bmatrix}, \mathbf{G_y} = \begin{bmatrix} \mathbf{2} & \mathbf{1} & \mathbf{0} & \mathbf{-1} & \mathbf{-2} \\ \mathbf{2} & \mathbf{1} & \mathbf{0} & \mathbf{-1} & \mathbf{-2} \\ \mathbf{4} & \mathbf{2} & \mathbf{0} & \mathbf{-2} & \mathbf{-4} \\ \mathbf{2} & \mathbf{1} & \mathbf{0} & \mathbf{-1} & \mathbf{-2} \\ \mathbf{2} & \mathbf{1} & \mathbf{0} & \mathbf{-2} & \mathbf{-2} \end{bmatrix} \quad (\mathbf{2})$$

The Kirsch operator consists of eight basic convolution kernels components [8]. However, the vertical and horizontal edges can be obtained using the 5×5 Gx and Gy kernels in equation (3).

$$\mathbf{G_x} = \begin{bmatrix} \mathbf{9} & \mathbf{9} & \mathbf{9} & \mathbf{9} & \mathbf{9} \\ \mathbf{9} & \mathbf{5} & \mathbf{5} & \mathbf{5} & \mathbf{9} \\ \mathbf{-7} & \mathbf{-3} & \mathbf{0} & \mathbf{-3} & \mathbf{-7} \\ \mathbf{-7} & \mathbf{-3} & \mathbf{-3} & \mathbf{-3} & \mathbf{-7} \\ \mathbf{-7} & \mathbf{-7} & \mathbf{-7} & \mathbf{-7} & \mathbf{-7} \end{bmatrix}, \mathbf{G_y} = \begin{bmatrix} \mathbf{9} & \mathbf{9} & \mathbf{-7} & \mathbf{-7} & \mathbf{-7} \\ \mathbf{9} & \mathbf{5} & \mathbf{-3} & \mathbf{-3} & \mathbf{-7} \\ \mathbf{4} & \mathbf{2} & \mathbf{0} & \mathbf{-3} & \mathbf{-7} \\ \mathbf{2} & \mathbf{1} & \mathbf{-3} & \mathbf{-3} & \mathbf{-7} \\ \mathbf{-2} & \mathbf{-2} & \mathbf{-7} & \mathbf{-7} & \mathbf{-7} \end{bmatrix} \quad (\mathbf{3})$$

The canny edge detector is an optimal approach to find the edges in images using a Gaussian filter to reduce noise when the raw image is convolved with this filter [23]. The masks in equation (5) implement 5×5 canny edge detection.

$$\mathbf{G_x} = \begin{bmatrix} \mathbf{15} & \mathbf{69} & \mathbf{114} & \mathbf{69} & \mathbf{15} \\ \mathbf{35} & \mathbf{155} & \mathbf{255} & \mathbf{155} & \mathbf{35} \\ \mathbf{0} & \mathbf{0} & \mathbf{0} & \mathbf{0} & \mathbf{0} \\ \mathbf{-35} & \mathbf{-155} & \mathbf{-255} & \mathbf{-155} & \mathbf{-35} \\ \mathbf{-15} & \mathbf{-69} & \mathbf{-144} & \mathbf{-69} & \mathbf{-15} \end{bmatrix}, \mathbf{G_{y=}} \begin{bmatrix} \mathbf{15} & \mathbf{35} & \mathbf{0} & \mathbf{-35} & \mathbf{-15} \\ \mathbf{69} & \mathbf{155} & \mathbf{0} & \mathbf{155} & \mathbf{69} \\ \mathbf{114} & \mathbf{255} & \mathbf{0} & \mathbf{-255} & \mathbf{-114} \\ \mathbf{69} & \mathbf{155} & \mathbf{0} & \mathbf{155} & \mathbf{69} \\ \mathbf{15} & \mathbf{35} & \mathbf{0} & \mathbf{35} & \mathbf{15} \end{bmatrix} \quad (\mathbf{4})$$

The second-order gradient Laplacian of Gaussian (LoG) edge detector can be used by convoluting the LoG filter to the image [24]. The mask in equation (5) implements the LoG filter.

$$\mathbf{G_x} = \begin{bmatrix} \mathbf{0} & \mathbf{0} & \mathbf{-1} & \mathbf{0} & \mathbf{0} \\ \mathbf{0} & \mathbf{-1} & \mathbf{-2} & \mathbf{-1} & \mathbf{0} \\ \mathbf{-1} & \mathbf{-2} & \mathbf{16} & \mathbf{0} & \mathbf{-1} \\ \mathbf{0} & \mathbf{-1} & \mathbf{-2} & \mathbf{-1} & \mathbf{0} \\ \mathbf{0} & \mathbf{0} & \mathbf{-1} & \mathbf{0} & \mathbf{0} \end{bmatrix} \quad (\mathbf{5})$$

4 Experimental Results

All the tests were done using a number of images similar to the images shown in Fig. 3 (a). This set of images was chosen as they had a mixture of surfaces all at varying depths and background with similar colour. All the images submitted as test results are the actual clinical images and photographed using a digital camera. The photographs were resized but not altered in any other way. The contribution each colour component made with respect to edge detection using both operators as shown in equation 4, the amount of noise, and the sharpness of the images were considered. Referring to Fig. 3 (b), it can be noted that the Sobel operator generated accurate edges; however, it was found that other operators such as Prewitt and canny operator can generate less noise.

The proposed method was implemented and tested on the processing system of ZYNQ-7000 (ARM processor) using the original OpenCV functions. Due to low speed performance of the processor, the same algorithm was implemented on FPGA side of ZYNQ using VIVADO HLS and XILINX Video Library. It should be noted that the current version of VIVADO HLS tool takes the advantage of a limited number of synthesizable OpenCV

functions which is used to develop the border detection IP. Fig. 3 illustrates the border detection result applied on clinical images. The output results tested on zc702 evaluation board with achieving not only the same imaging results as ARM processor but also with a higher speed of 60 fps. In addition, the results for Sobel, Kirsch, LoG and Canny edge-detection implementations are compared. The results showed that the extended 5×5 canny edge detection has better performance than other methods.

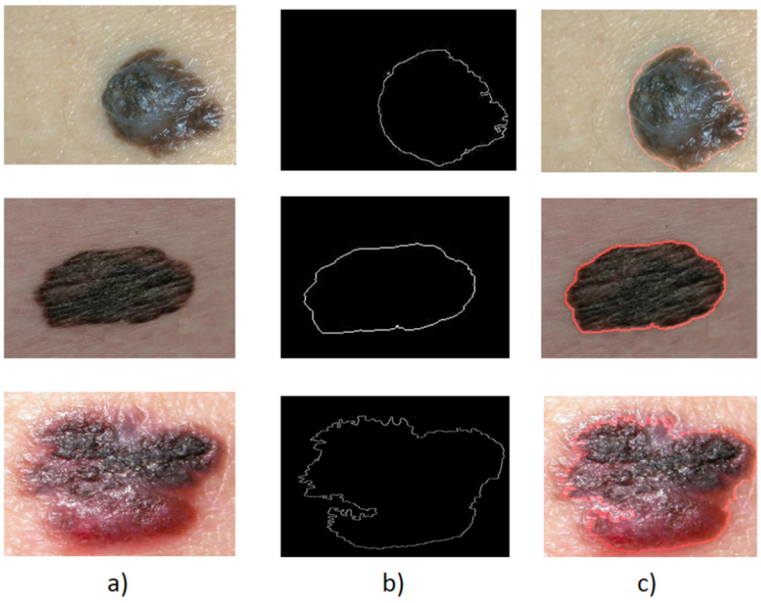

Fig. 3. Border detection results. (a) Original clinical images, (b) Result of border detection using VIVADO HLS, (c) Matching the detected border on the original image.

5 Conclusions

The effect of applying morphological filters and edge detection algorithms on skin lesion images in order to detect border of PSLs is discussed using ZYNQ-7000 single SoC. The results show that the extended 5×5 canny edge detection implemented on the proposed embedded platform has better performance than other reported methods. Consequently, it can segment the lesion as it is important step before image analysis and feature extraction for melanoma detection. Moreover, using C-to-FPGA technology and VIVADO HLS software, we can increase productivity and performance of the system compared with current FPGA programming approaches.
However, there is a trade-off between strong edge detection and noise, this is apparent when comparing the Sobel and Prewitt operators. It was found that pre-processing of the image may, in some circumstances; result in less noise on the output. Synthesising the IP used in this application allows a real time result. This is achieved by the fact that edge detection IP is working in parallel for RGB images. The throughput is achieved by running processes in parallel rather than all out speed. Employing other optimisation techniques for the image analysis can enhance the performance. The advancement in high definition media in recent years, high–speed embedded systems and the growth of applications in healthcare systems provide the opportunity to revolutionize the skin cancer diagnosis. In this work, using the state of the art FPGA technology as an example, we implemented the fundamental image processing algorithms on a SoC and demonstrated its rapid processing power that supports such transition.

References

[1] T. Diepgen and V. Mahler, "The Epidemiology of Skin Cancer," *British Journal of Dermatology*, Vol. 146, pp. 1-6, 2002.

[2] L. A. Goldsmith, F. B. Askin, A. E. Chang, C. Cohen, J. P. Dutcher, R. S. Gilgor, S. Green, E. L. Harris, S. Havas, and J. K. Robinson, "Diagnosis and Treatment of Early Melanoma," *The Journal of the American Medical Association*, Vol. 268, pp. 1314-1319, 1992.

[3] K. Konstantin and G. Rafael, "Computerized Analysis of Pigmented Skin Lesions: A Review," *Artificial Intelligence in Medicine,* Vol. 56, 2012.

[4] A. Sahu, C. McGoverin, N. Pleshko, K. Sorenmo, C.-H. Won, "Hyperspectral Imaging System to Discern Malignant and Benign Canine Mammary Tumors," in *Proceedings of SPIE Defense, Security, and Sensing*, pp. 87190W-87190W-8, 2013.

[5] S. Kiyotoki, J. Nishikawa, T. Okamoto, K. Hamabe, M. Saito, A. Goto, Y. Fujita, Y. Hamamoto, Y. Takeuchi, S. Satori, "New Method for Detection of Gastric Cancer by Hyperspectral Imaging: A Pilot Study," *Journal of Biomedical Optics*, Vol. 18, pp. 026010-026010, 2013.

[6] G. Argenziano, H. P. Soyer, S. Chimenti, R. Talamini, R. Corona, F. Sera, M. Binder, L. Cerroni, G. De Rosa, G. Ferrara, "Dermoscopy of Pigmented Skin Lesions: Results of a Consensus Meeting via the Internet," *Journal of the American Academy of Dermatology*, Vol. 48, p. 679, 2003.

[7] L. Xu, M. Jackowski, A. Goshtasby, D. Roseman, S. Bines, C. Yu, A. Dhawan, A. Huntley, "Segmentation of Skin Cancer Images," *Image and Vision Computing*, Vol. 17, pp. 65-74, 1999.

[8] A. Jukić, I. Kopriva, A. Cichocki, "Noninvasive Diagnosis of Melanoma with Tensor Decomposition-Based Feature Extraction from Clinical Color Image," *Biomedical Signal Processing and Control*, Vol. 8, pp. 755-763, 2013.

[9] M. S. Mabrouk, M. Sheha, and A. A. Sharawy, "Computer Aided Diagnosis of Melanoma Skin Cancer Using Clinical Photographic Images," *International Journal of Computers & Technology*, Vol. 10, pp. 1922-1929, 2013.

[10] R. Dobai and L. Sekanina, "Towards Evolvable Systems Based on the Xilinx Zynq Platform," in *Proceedings of 2013 IEEE International Conference on Evolvable Systems*, pp. 89-95, 2013.

[11] J. Chen, J. Cong, M. Yan, Y. Zou, "FPGA-accelerated 3D Reconstruction Using Compressive Sensing," in *Proceedings of the ACM/SIGDA international symposium on Field Programmable Gate Arrays*, pp. 163-166, 2012.

[12] J. Noguera, S. Neuendorffer, S. Van Haastregt, J. Barba, K. Vissers, C. Dick, "Implementation of Sphere Decoder for MIMO-OFDM on FPGAs Using High-level Synthesis Tools," *Analog Integrated Circuits and Signal Processing,* Vol. 69, pp. 119-129, 2011.

[13] J. Cong, P. Zhang, Y. Zou, "Combined Loop Transformation and Hierarchy Allocation for Data Reuse Optimization," in *Proceedings of 2011 IEEE/ACM International Conference on Computer-Aided Design (ICCAD)*, pp. 185-192, 2011.

[14] G. Sapiro, "Segmenting Skin Lesions with Partial-differential-equations-based Image Processing Algorithms," *IEEE Transactions on Medical Imaging,* Vol. 19, pp. 763-767, 2000.

[15] H. Ganster, P. Pinz, R. Rohrer, E. Wildling, M. Binder, H. Kittler, "Automated Melanoma Recognition," *IEEE Transactions on Medical Imaging*, Vol. 20, pp. 233-239, 2001.

[16] J. Tang, "A Multi-direction GVF Snake for the Segmentation of Skin Cancer Images," *Pattern Recognition*, Vol. 42, pp. 1172-1179, 2009.

[17] R. Garnavi, M. Aldeen, M. E. Celebi, G. Varigos, S. Finch, "Border Detection in Dermoscopy Images Using Hybrid Thresholding on Optimized Color Channels," *Computerized Medical Imaging and Graphics*, Vol. 35, pp. 105-115, 2011.

[18] M. E. Celebi, G. Schaefer, H. Iyatomi, W. V. Stoecker, "Lesion Border Detection in Dermoscopy Images," *Computerized Medical Imaging and Graphics*, Vol. 33, p. 148, 2009.

[19] P. Wighton, T. K. Lee, H. Lui, D. I. McLean, M. S. Atkins, "Generalizing Common Tasks in Automated Skin Lesion Diagnosis," *IEEE Transactions on Information Technology in Biomedicine*, Vol. 15, pp. 622-629, 2011.

[20] Q. Abbas, M. E. Celebi, I. Fondón García, M. Rashid, "Lesion Border Detection in Dermoscopy Images Using Dynamic Programming," *Skin Research and Technology*, Vol. 17, pp. 91-100, 2011.

[21] M. Setayesh, Z. Mengjie, M. Johnston, "Effects of Static and Dynamic Topologies in Particle Swarm Optimisation for Edge Detection in Noisy Images," in *Proceedings of 2012 IEEE Congress on Evolutionary Computation (CEC 2012)*, pp. 1-8, 2012.

[22] D. H. B. Kekre and M. S. M. Gharge, "Image Segmentation Using Extended Edge Operator for Mammographic Images," *International journal on computer science and Engineering*, vol. 2, pp. 1086-1091, 2010.

[23] J. Canny, "A Computational Approach to Edge Detection," *IEEE Transactions on Pattern Analysis and Machine Intelligence*, Vol. PAMI-8, pp. 679-698, 1986.

[24] A. P. Dhawan, *Medical Image Analysis*, 2nd Edition, Wiley-IEEE Press, 2011.